Evolution of the Southern Annular Mode during the last millennium

Nerilie J. Abram[1,2*], Robert Mulvaney[1], Françoise Vimeux[3], Steven J. Phipps[4], John Turner[1] and Matthew H. England[4]

1. British Antarctic Survey, Natural Environment Research Council, Cambridge CB3 0ET, United Kingdom
2. Research School of Earth Sciences, Australian National University, Canberra ACT 0200, Australia
3. Institut de Recherche pour le Développement, Laboratoire HydroSciences Montpellier et Laboratoire des Sciences du Climat et de l'Environment, 91191 Gif-sur-Yvette, France
4. Climate Change Research Centre and ARC Centre of Climate System Science, University of New South Wales, Sydney NSW 2052, Australia
*email: nerilie.abram@anu.edu.au

The Southern Annular Mode (SAM) is the primary pattern of climate variability in the Southern Hemisphere[1,2], influencing latitudinal rainfall distribution and temperatures from the subtropics to Antarctica. The positive summer trend in the SAM over recent decades is widely-attributed to stratospheric ozone depletion[2], however the brevity of observational records from Antarctica[1] – one of the core zones that defines SAM variability – limits our understanding of long-term SAM behaviour. Here we reconstruct annual-mean changes in the SAM since 1000AD using, for the first time, proxy records that encompass the full mid-latitude to polar domain across the Drake Passage sector. We find that the SAM has undergone a progressive shift towards its positive phase since the 15th Century, causing cooling of the main Antarctic continent at the same time that the Antarctic Peninsula has warmed. The positive trend in the SAM since ~1940AD is reproduced by multi-model climate simulations forced with rising greenhouse gas levels and later ozone depletion, and the long-term average SAM Index is now at its highest level for at least the last 1000 years. Reconstructed SAM trends prior to the 20th Century are more prominent than those in radiative-forcing climate experiments, and may be associated with a teleconnected response to tropical Pacific climate. Our findings imply that predictions of further greenhouse-driven increases in the SAM over the coming century[3] also need to account for the possibility of opposing effects from tropical Pacific climate changes.

Warming of the polar-regions has global implications for sea level rise and climate change feedback processes such as decreased planetary albedo and the release of naturally-stored carbon reservoirs. High latitude amplification of global warming trends is clearly observed across the Arctic[4,5]. In contrast, Antarctica is the only continental region where long-term cooling over the last 2000 years has not yet been reversed to climate warming[5]. Yet some regions of Antarctica have warmed significantly over the last ~50 years, with the Antarctic Peninsula and parts of West Antarctica displaying the most rapid temperature increases in the Southern Hemisphere[6,7]. Understanding these regional responses of Antarctic temperature to recent climate change requires an improved characterisation of natural and anthropogenically-driven changes in Southern Hemisphere climate variability.

In this study we use the James Ross Island (JRI) ice core from the northern Antarctic Peninsula[7-9] (64.2^{o}S, 57.7^{o}W; Fig. 1), along with other published temperature-sensitive proxies[5], to reconstruct Southern Annular Mode (SAM) variability since 1000AD. The SAM can be defined by the zonal mean atmospheric pressure difference between the mid-latitudes (~40^{o}S) and Antarctica (~65^{o}S)[1]. The positive phase of the SAM is associated with low pressure anomalies over Antarctica and high pressure anomalies over the mid-latitudes, and this enhanced atmospheric pressure gradient results in strengthening and poleward contraction of the Southern Hemisphere westerly jet stream[1]. The mountainous geographic barrier of the Antarctic Peninsula makes temperature variability in this region particularly sensitive to the strength of the westerly winds passing through Drake Passage. As such, JRI is a key location for documenting SAM-related climate variability (Fig. 1b) and previous work[8,9] has demonstrated that the water isotope-derived temperature record from the JRI ice core is significantly correlated with observational indices of the SAM[1,10].

The JRI temperature record since 1000AD has an inverse correlation with the PAGES2k reconstruction of continental Antarctic temperature[5] (Fig. 1a). This opposing temperature history between the Antarctic Peninsula and the main Antarctic continent is consistent with the spatial response of surface air temperatures to SAM variability (Fig. 1b), and is statistically significant at annual to multi-decadal timescales (Table 1). The JRI temperature record also displays similarities to the PAGES2k South American temperature reconstruction[5] that may indicate a shared climate forcing, although the positive correlation between the two datasets is not statistically significant

(Table 1). However, in their long-term evolution the South American and JRI reconstructions both indicate that the coolest 50-year interval of the last millennium occurred at 1410-1460AD, with progressive phases of warming since that time (Fig. 1a).

We combine the JRI temperature record with the PAGES2k compilations of South American and Antarctic temperature-sensitive proxies to derive a weighted composite-plus-scale[11,12] reconstruction of the SAM Index during the last millennium (Fig. 2; Methods; Supplementary Table 1; Supplementary Figures 1-3). Together, the proxies capture climate information in all seasons and span the mid-latitude to polar domains where the SAM has a major influence on temperature (Fig. 1b). Multi-model climate simulations indicate that the regional temperature patterns associated with modern-day SAM variability persisted through the last millennium (Supplementary Figure 4), supporting the use of the proxy network to reconstruct the long-term history of the SAM. We restrict the mid-latitude proxy data to the South American continent to produce a reconstruction that is specifically related to SAM variability in the Drake Passage sector. We do this because although the SAM is classically described as a zonally-symmetric climate feature, its variability and tropical climate interactions have seasonal asymmetries that are particularly strong in the South Pacific and Antarctic Peninsula regions[13-15]. Analysis with ERA-Interim[16] data since 1979AD and climate simulations spanning the last millennium demonstrates, however, that at annual average and longer timescales SAM variability in the Drake Passage sector is highly representative of the circumpolar mean state of the SAM (Supplementary Figures 5-6).

Our SAM reconstruction for the last millennium shows that the most extreme negative phase of the SAM occurred during the 15th Century (Fig. 2c, Fig. 3a). Other proxy-based assessments support a minimum in the SAM at this time. For example, an epoch-analysis of proxies for Southern Hemisphere circulation identified persistent negative SAM conditions between 1300 – 1450AD[17], while a 600-year reconstruction based on mid-latitude tree growth in New Zealand and South America documented the most extreme negative summer SAM values at ~1470AD[18] (Fig 3b). A 700-year winter sea salt record from the Law Dome ice core also shows a tendency for more positive SAM conditions since ~1500AD[19], and an increase in the frequency of severe droughts in the Central Andes over the last six centuries has been attributed to southward contraction of the westerly storm tracks[20] (Supplementary Figure 7). Together these records demonstrate that the positive

trend in SAM since the 15th Century is a robust feature that impacted mid-latitude and polar sites around the full SAM domain.

Our reconstruction indicates that the transition to a more positive SAM after the 15th Century occurred in two stages. First, a progressive increase in the SAM occurred during the ~300 years spanning the 16th to 18th Centuries. This trend then reversed during the 19th Century, before recommencing in the 20th century (Fig. 2c). Trend analysis tests on our proxy-based reconstruction indicate that the recent positive trend in the annual SAM Index has been significant since ~1940AD (Supplementary Figure 8a).

A valuable tool to assess proxy-model agreement on past SAM behavior are the "last millennium" transient climate model simulations performed as part of the 5th Coupled Model Intercomparison Project (CMIP5)[21,22] (methods; Supplementary Table 2). The ensemble mean of eight climate models indicates that the positive SAM trend during the 20th Century is a feature that is consistently produced in experiments with transient radiative forcings (Fig. 3c,d). The positive trend in the modeled SAM Index since 1940AD has an equivalent magnitude (+0.3 units/decade) to our proxy-based reconstruction, although the precise initiation point for the 20th Century SAM increase is not as well-constrained in the CMIP5 ensemble mean (Supplementary Figure 8). This is because the CMIP5 simulations do not reproduce the negative SAM trend during the 19th Century that is observed in the proxy-derived reconstruction. The CMIP5 ensemble mean also displays a much weaker positive trend in the SAM Index during the 16th to 18th Centuries (+0.006 units/decade) than indicated by our reconstruction (+0.1 units/decade). Thus, while proxy-model agreement on SAM trends in the 20th century is reasonably good, there are discrepancies in the structure and magnitude of SAM changes prior to this time.

The influence of different radiative forcing mechanisms on the evolution of SAM is investigated using multiple simulations of the last millennium with a coupled climate model[23] (Methods; Fig. 3e). No long-term trend in the SAM is observed in experiments conducted using only orbital forcing. The addition of anthropogenic greenhouse gases causes a positive shift in the ensemble mean SAM Index that exceeds the +2σ level of unforced SAM variability during the 20th Century. This is in

agreement with other model-based studies that find increased greenhouse gas levels cause a positive shift in the SAM due to enhanced meridional temperature gradients in the Southern Hemisphere[2,3]. It is also consistent with the hypothesis that the early-mid 20th century commencement of Antarctic Peninsula warming is not explained by ozone-forced increases of the SAM alone[9].

The addition of solar forcing to the coupled climate model simulations produces an increasing trend in the SAM Index over the 16th to 18th Centuries (Fig. 3e). This could be explained by increasing solar irradiance after the 15th Century Spörer minimum, as multi-model assessments of CMIP5 historical simulations (since 1861AD) have determined that changes in solar irradiance exert a small positive forcing on the SAM[3]. However, the modeled SAM trend during the 16th to 18th Centuries is not significant relative to the distribution of trends in a 10,000-year unforced simulation of the same model. The large pre-industrial trends in SAM that are suggested by proxy records may thus imply that the SAM is more responsive to direct solar forcing than indicated by current climate simulations[3], or that the magnitude of solar irradiance changes applied in the last millennium simulations is too low[24,25]. Further modeling studies using the full range of solar irradiance change estimates[25] may help to clarify the impact that past solar changes had on the SAM. Alternately, it is possible that proxy-based reconstructions overestimate the magnitude of long-term changes in the SAM, or that the long-term changes in the SAM prior to anthropogenic greenhouse and ozone forcing were caused by internal variability or other physical process that cannot be resolved in radiative-forcing experiments.

Tropically-forced climate variability projects upon the high-latitude SAM pattern in the Drake Passage sector and may provide an additional mechanism to explain SAM trends during the last millennium. Instrumental studies have shown that El Niño-Southern Oscillation (ENSO) variability in the tropical Pacific interacts via a Rossby wave-train with storm tracks in the South Pacific, such that El Niño (La Niña) events tend to cause cool (warm) conditions on the Antarctic Peninsula (Fig. 4a) and are associated with negative (positive) SAM states[13-15]. Using a recent multivariate reconstruction of SST in the Niño3.4 region since 1150AD[26], a significant inverse correlation with our SAM reconstruction is obtained (Table 1). It is noted, however, that the Niño3.4 reconstruction also draws upon tree-growth records from South America. Therefore, we further verify that a significant

inverse relationship exists between the Niño3.4 reconstruction and the independent JRI temperature record, located in the core region of ENSO-SAM teleconnections (Fig. 4; Table 1; Supplementary Figure 9). This suggests that the association of El Niño with negative SAM states is likely to be a persistent feature of the long-term interaction of these climate modes in the Antarctic Peninsula region.

If the ENSO-SAM relationship that exists on interannual timescales also influences the mean state of these climate modes, then the maximum in Niño3.4 SSTs during the 15th century[26] could have contributed to the SAM minimum at this time (Fig. 4b). The positive trend in Antarctic Peninsula temperature and the SAM during the 16th to 18th Centuries, and the reversal of these changes during the 19th Century, also closely mirror changes in mean Niño3.4 SST. However, tropical Pacific climate appears to become a secondary influence on SAM trends during the 20th Century, when the positive trend in Niño3.4 SST[26] would be expected to have imposed a negative forcing on the mean state of SAM in the Drake Passage sector. A recent study highlighted that the positive trend in summer SAM during the 20th Century has emerged above the opposing interannual forcing by ENSO[27]. Our findings extend this perspective over the last millennium, and suggest that tropical Pacific SST trends could have acted in a way that has muted the impact of increasing greenhouse gases and ozone depletion on SAM during the 20th Century.

The long-term mean of the SAM Index is now at its highest positive value for at least the last 1000 years (Fig. 2c). Continued increases in atmospheric greenhouse gases are predicted to force the SAM further towards its positive phase over the coming century[2,3]. At the same time, stratospheric ozone recovery is expected to cause an opposing effect that may limit the magnitude of the positive greenhouse-driven SAM trend in summer[2,3]. However, summer temperatures along the Antarctic Peninsula are already sufficiently high to cause extensive surface ice melt[9], and SAM-driven warming in other seasons may further increase the duration of the melt season along the Antarctic Peninsula[28]. Future greenhouse-driven increases in the SAM are also likely to have implications for limiting warming over continental Antarctica[5] and for southward expansion of the dry sub-tropical climate belts[18,20]. In addition, the tropical Pacific is predicted to experience more extreme El Niño events during the coming century[29] and our findings highlight the importance of being able to accurately model how their remote climate teleconnections will also impact the SAM.

Methods

Proxy records. We use the deuterium isotope record from the James Ross Island ice core as a temperature proxy for the Antarctic Peninsula region[8,9]. Full details of the ice core site and isotope analysis can be found in ref. 7. We use the JRI1 age model with annual layer chronology since 1807, as in ref. 9. Deuterium isotope measurements made at 10cm resolution along the upper 300m of the ice core correspond to better than annual resolution since 1111AD, and were binned to produce annual (~January-December) averages. The 111 years between 1000-1110AD comprise 85 isotope measurements and interpolation was used to generate a pseudo-annual resolution record over this interval.

We also use temperature-sensitive proxy records for the Antarctic and South America continental regions[5] to capture the full mid-latitude to polar expression of the SAM across the Drake Passage transect. The annually-resolved proxy datasets compiled as part of the PAGES2k database are published and publically available[5]. For the South American dataset we restrict our use to records south of 30^{o}S and we do not use the four shortest records that are derived from instrumental sources. Details of the individual records used in this study and their correlation with the SAM are given in Supplementary Table 1.

Data available at ftp://ftp.ncdc.noaa.gov/pub/data/paleo/icecore/antarctica/james-ross-island/ and http://www.nature.com/ngeo/journal/v6/n5/full/ngeo1797.html

SAM reconstruction. The proxy records from the South America, Antarctic Peninsula and Antarctic continent regions (where SAM has a significant influence on temperature; Fig. 1b) were used to reconstruct an annual average SAM Index since 1000AD. We employ the widely-used Composite-Plus-Scale (CPS) methodology[5,11,12] with nesting to account for the varying length of proxies making up the reconstruction. For each nest the contributing proxies were normalised relative to the 1957-1995AD calibration interval, which represents the interval of maximum overlap between the annual (Jan-Dec) Marshall-SAM Index (http://www.antarctica.ac.uk/met/gjma/sam.html) and the majority of the proxy network (Supplementary Table 1). The normalised proxy records were then combined with a weighting[12] based on their correlation coefficient (r) with the SAM during the calibration interval (Supplementary Table 1). The combined record was then scaled to match the mean and standard deviation of the instrumental SAM Index during the calibration interval. Finally, nests were spliced together to provide the full 1000-year SAM reconstruction. Alternate methods for carrying out the CPS reconstruction were explored and the primary findings discussed in this study are shown to be robust across different methodologies (Supplementary Figures 1-2).

For each proxy nest a 95% confidence interval was defined as 1.96 times the standard deviation of the residuals of the SAM reconstruction from Marshall-SAM Index during the calibration interval. The reduction of error (RE) statistic was also calculated to test the performance of the reconstruction. The brevity of Antarctic instrumental records limits the ability to cross validate the SAM reconstruction using separate calibration and verification intervals[18]. Instead, we assess the significance of RE values by repeating 1000 CPS simulations where the proxy network was replaced by AR(1) time series matching the length and lag-1 autocorrelation of the proxies, and we use the upper 95th percentile to determine the critical RE level (RE_{crit}) for each proxy nest. We further verify the SAM reconstruction against the extended Fogt-SAM Index[10] (http://polarmet.osu.edu/ACD/sam/sam_recon.html). To perform this

assessment the four seasonal reconstructions of the Fogt-Index were averaged to estimate an annual (Dec-Nov) SAM, which was then scaled to match the variance of the Marshall-SAM Index from 1961-1990.

Model output. We use multi-model output from the subset of CMIP5 climate models that ran transient last millennium (past1000) simulations since 850AD[21,22]. Historical simulations from the same ensemble were used to extend the model output from 1850AD. The CMIP5 past1000 and historical experiments use transient radiative forcings that include orbital, solar, volcanic, greenhouse and ozone parameters as well as land use changes[21,22]. All data was accessed from the Earth System Grid Federation node (http://pcmdi9.llnl.gov/esgf-web-fe/), with the exception of the historical portion of the HadCM3 last millennium simulation (provided by Andrew Schurer, Edinburgh University) and the CSIRO Mk3L simulations. To assess the importance of different radiative forcing mechanisms, we used multiple simulations of the last 1500 years performed with the CSIRO Mk3L coupled climate model, as described in ref. 23. Supplementary Table 2 gives further details on the climate model datasets.

In this study we utilise monthly resolution mean sea level pressure (psl) data to calculate the zonal mean at 40^{o}S and 65^{o}S. The model-generated data were averaged into January-December annuals to match the proxy data, normalised relative to the 1961-1990AD interval and differenced to generate a SAM Index[1]. We also use surface air temperature (tas) model output to examine SAM-temperature relationships at our proxy sites in the last millennium climate simulations (Supplementary Figure 4).

Data archive. The SAM reconstruction developed in this paper is archived with the World Data Center for Paleoclimatology (http://hurricane.ncdc.noaa.gov/pls/paleox/f?p=519:1:::::P1_STUDY_ID:16197).

Acknowledgements

N.J.A. is supported by a Queen Elizabeth II fellowship awarded by the Australian Research Council (ARC DP110101161). This study contributes to ARC Discovery Project DP140102059 awarded to N.J.A. and R.M., and is part of the British Antarctic Survey "Polar Science for Planet Earth" programme funded by the Natural Environment Research Council. Modelling work using CSIRO Mk3L was supported by an award to S.J.P. of computational resources on the NCI National Facility through the National Computational Merit Allocation Scheme. M.H.E. is supported by ARC Laureate Fellowship FL100100214. We thank Eric Wolff for discussions that improved the paper, and we gratefully acknowledge the efforts of the PAGES2k and CMIP5/PMIP3 communities in archiving the proxy synthesis and model products that were utilised in this study.

Author Contributions

N.J.A. conceived the study and performed the data analysis, with support from the other authors. All authors contributed to the discussion of ideas and writing of the paper.

Additional information

Supplementary information is available in the online version of the paper. Reprints and permissions information is available online at www.nature.com/reprints. Correspondence and requests for materials should be addressed to N.J.A.

Competing financial interests

The authors declare no competing financial interests.

References

1 Marshall, G. J. Trends in the southern annular mode from observations and reanalyses. *J. Clim.* **16**, 4134-4143 (2003).

2 Thompson, D. W. J. *et al.* Signatures of the Antarctic ozone hole in Southern Hemisphere surface climate change. *Nature Geosci.* **4**, 741-749 (2011).

3 Gillett, N. P. & Fyfe, J. C. Annular mode changes in the CMIP5 simulations. *Geophys. Res. Lett.* **40**, 1189-1193, doi:10.1002/grl.50249 (2013).

4 Screen, J. A. & Simmonds, I. The central role of diminishing sea ice in recent Arctic temperature amplification. *Nature* **464**, 1334-1337, doi:10.1038/nature09051 (2010).

5 PAGES 2k consortium. Continental-scale temperature variability during the past two millennia. *Nature Geosci.* **6**, 339-346, doi:10.1038/ngeo1797 (2013).

6 Bromwich, D. H. *et al.* Central West Antarctica among the most rapidly warming regions on Earth. *Nature Geosci.* **6**, 139-144, doi:10.1038/ngeo1671 (2013).

7 Mulvaney, R. *et al.* Recent Antarctic Peninsula warming relative to Holocene climate and ice-shelf history. *Nature* **489**, 141-144 (2012).

8 Abram, N. J., Mulvaney, R. & Arrowsmith, C. Environmental signals in a highly resolved ice core from James Ross Island, Antarctica. *J. Geophys. Res.* **116**, D20116, doi:10.1029/2011jd016147 (2011).

9 Abram, N. J. *et al.* Acceleration of snow melt in an Antarctic Peninsula ice core during the twentieth century. *Nature Geosci.* **6**, 404-411, doi:10.1038/ngeo1787 (2013).

10 Fogt, R. L. *et al.* Historical SAM Variability. Part II: Twentieth-Century Variability and Trends from Reconstructions, Observations, and the IPCC AR4 Models. *J. Clim.* **22**, 5346-5365, doi:10.1175/2009jcli2786.1 (2009).

11 Jones, P. D. *et al.* High-resolution palaeoclimatology of the last millennium: a review of current status and future prospects. *The Holocene* **19**, 3-49, doi:10.1177/0959683608098952 (2009).

12 Hegerl, G. C. *et al.* Detection of human influence on a new, validated 1500-year temperature reconstruction. *J. Clim.* **20**, 650-666, doi:10.1175/JCLI4011.1 (2007).

13 Ding, Q. H., Steig, E. J., Battisti, D. S. & Wallace, J. M. Influence of the Tropics on the Southern Annular Mode. *J. Clim.* **25**, 6330-6348, doi:10.1175/jcli-d-11-00523.1 (2012).

14 Fogt, R. L., Jones, J. M. & Renwick, J. Seasonal Zonal Asymmetries in the Southern Annular Mode and Their Impact on Regional Temperature Anomalies. *J. Clim.* **25**, 6253-6270, doi:10.1175/jcli-d-11-00474.1 (2012).

15 Fogt, R. L., Bromwich, D. H. & Hines, K. M. Understanding the SAM influence on the South Pacific ENSO teleconnection. *Clim. Dynam.* **36**, 1555-1576, doi:10.1007/s00382-010-0905-0 (2011).

16 Dee, D. P. *et al.* The ERA-Interim reanalysis: configuration and performance of the data assimilation system. *Q. J. R. Meteorol. Soc.* **137**, 553-597, doi:10.1002/qj.828 (2011).

17 Goodwin, I. *et al.* A reconstruction of extratropical Indo-Pacific sea-level pressure patterns during the Medieval Climate Anomaly. *Clim. Dynam.*, 1-23, doi:10.1007/s00382-013-1899-1 (2013).

18 Villalba, R. *et al.* Unusual Southern Hemisphere tree growth patterns induced by changes in the Southern Annular Mode. *Nature Geosci.* **5**, 793-798, doi:10.1038/ngeo1613 (2012).

19 Goodwin, I. D., van Ommen, T. D., Curran, M. A. J. & Mayewski, P. A. Mid latitude winter climate variability in the South Indian and southwest Pacific regions since 1300 AD. *Clim. Dynam.* **22**, 783-794, doi:10.1007/s00382-004-0403-3 (2004).

20 Christie, D. A. *et al.* Aridity changes in the Temperate-Mediterranean transition of the Andes since ad 1346 reconstructed from tree-rings. *Clim. Dynam.* **36**, 1505-1521, doi:10.1007/s00382-009-0723-4 (2011).

21 Taylor, K. E., Stouffer, R. J. & Meehl, G. A. An overview of CMIP5 and the experiment design. *Bull. Amer. Meteorol. Soc.* **93**, 485-498, doi:10.1175/bams-d-11-00094.1 (2012).

22 Schmidt, G. A. *et al.* Climate forcing reconstructions for use in PMIP simulations of the last millennium (v1.0). *Geosci. Model Dev.* **4**, 33-45, doi:10.5194/gmd-4-33-2011 (2011).

23 Phipps, S. J. *et al.* Paleoclimate data-model comparison and the role of climate forcings over the past 1500 years. *J. Clim.*, doi:10.1175/jcli-d-12-00108.1 (2013).

24 Shapiro, A. I. *et al.* A new approach to the long-term reconstruction of the solar irradiance leads to large historical solar forcing. *Astronomy and Astrophysics* **529**, A67, doi:10.1051/0004-6361/201016173 (2011).

25 Schmidt, G. A. *et al.* Climate forcing reconstructions for use in PMIP simulations of the last millennium (v1.1). *Geosci. Model Dev.* **5**, 185-191, doi:10.5194/gmd-5-185-2012 (2012).

26 Emile-Geay, J., Cobb, K. M., Mann, M. E. & Wittenberg, A. T. Estimating Central Equatorial Pacific SST Variability over the Past Millennium. Part II: Reconstructions and Implications. *J. Clim.* **26**, 2329-2352, doi:10.1175/jcli-d-11-00511.1 (2013).
27 Wang, G. J. & Cai, W. J. Climate-change impact on the 20th-century relationship between the Southern Annular Mode and global mean temperature. *Sci. Rep.* **3**, doi:2039. 10.1038/srep02039 (2013).
28 Barrand, N. E. *et al.* Trends in Antarctic Peninsula surface melting conditions from observations and regional climate modelling. *J. Geophys. Res.*, doi:10.1029/2012JF002559 (2013).
29 Cai, W. *et al.* Increasing frequency of extreme El Nino events due to greenhouse warming. *Nature Clim. Change* **4**, 111-116, doi:10.1038/nclimate2100 (2014).
30 Reynolds, R. W., Rayner, N. A., Smith, T. M., Stokes, D. C. & Wang, W. An improved in situ and satellite SST analysis for climate. *J. Clim.* **15**, 1609-1625 (2002).

Table 1. Correlation statistics for the time series.

Correlation series	annual averages	7y moving averages	70y moving averages
JRI temperature vs Antarctic2k temperature[5]	r = -0.055* n = 1006	r = -0.117*	r = -0.535***
JRI temperature vs South America2k temperature[5]	r = 0.008 n = 996	r = 0.075	r = 0.247
SAM reconstruction vs Niño3.4 reconstruction[26]	r = -0.074** n = 846	r = -0.163**	r = -0.328*
JRI temperature vs Niño3.4 reconstruction[26]	r = -0.077** n = 846	r = -0.189***	r = -0.379*

Significance indicated as: *p < 0.1, **p<0.05, and ***p<0.01, assessed using 1000 simulations of AR(1) noise with the same length and lag-1 autocorrelation as the datasets.

Figure captions

Figure 1. Regional temperature histories. a. JRI temperature reconstruction[7,9] (green) alongside continent-scale temperature reconstructions[5] for South America (red) and Antarctica (blue; excludes JRI). Anomalies shown as 7y (thin) and 70y (thick lines and grey shading) moving averages, relative to 1961-1990AD means (dashed). b, Location of JRI (green cross) and proxies used in the South America (red crosses) and Antarctica (blue crosses) temperature reconstructions. Shading shows spatial correlation ($p<0.1$) of the annual SAM Index[1] with 2m air temperature in the ERA-Interim reanalysis[16] (Jan-Dec averages; 1979-2012AD).

Figure 2. SAM reconstruction. a, Correlation of the proxy network to the annual (Jan-Dec) SAM Index[1] during 1957-1995AD calibration interval. b, SAM reconstruction (grey line and shading) alongside Marshall[1] (orange; 1957-2007AD) and Fogt[10] (purple; 1905-2005AD) SAM Indices. All records shown at annual resolution (thin) and 7y moving averages (thick), relative to 1961-1990AD mean (dashed). c, SAM reconstruction for the last millennium, as 7y moving average (thin grey) and 70y loess filter (thick black), with 95% confidence interval around the annual reconstruction (grey shading; with 70y loess smoothing), relative to 1961-1990AD mean (dashed black). Also shown are reduction of error (RE) statistics (teal solid; which remain above RE_{crit} (dashed; $p=0.05$)), the number of contributing proxies, and 7y moving averages of the Marshall (orange) and Fogt (purple) SAM Indices.

Figure 3. SAM data-model comparison. a, SAM reconstruction (black) compared with, b, a mid-latitude summer-SAM reconstruction[18] (brown); both as 7y moving averages (thin) and 70y loess filter (thick). c, Ensemble mean (red) SAM Index across multi-model CMIP5 simulations[21] (grey; 70y moving averages) using d, transient radiative forcing[22] (example from CSIRO-Mk3L[23], expressed relative to 1001-1200AD mean). SAM Indices (a-c) relative to 1961-1990AD means (dashed). e, CSIRO-Mk3L realisations of the SAM Index using progressive addition of radiative forcings[23]. Each curve represents the 3 ensemble average, as 70y moving averages relative to 1001-1200AD means (grey shading). Dashed lines show ±2σ range of internal variability based on orbital-only simulations.

Figure 4. ENSO teleconnections. a, Spatial correlation (Jan-Dec averages; 1982-2012AD; $p<0.1$) of Niño3.4 SST[30] with ERA-Interim[16] 2m temperature demonstrating phasing of El Niño (La Niña) states with cooling (warming) in the Antarctic Peninsula region[13]. Black rectangle shows Niño3.4 region, black square shows JRI location. b, SAM reconstruction (black) and JRI temperature (green), shown alongside a multiproxy reconstruction[26] of Niño3.4 SST (dark red). All shown as 7y moving averages (thin grey) and 70y loess filter (thick lines and grey shading), relative to 1961-1990AD means (dashed).

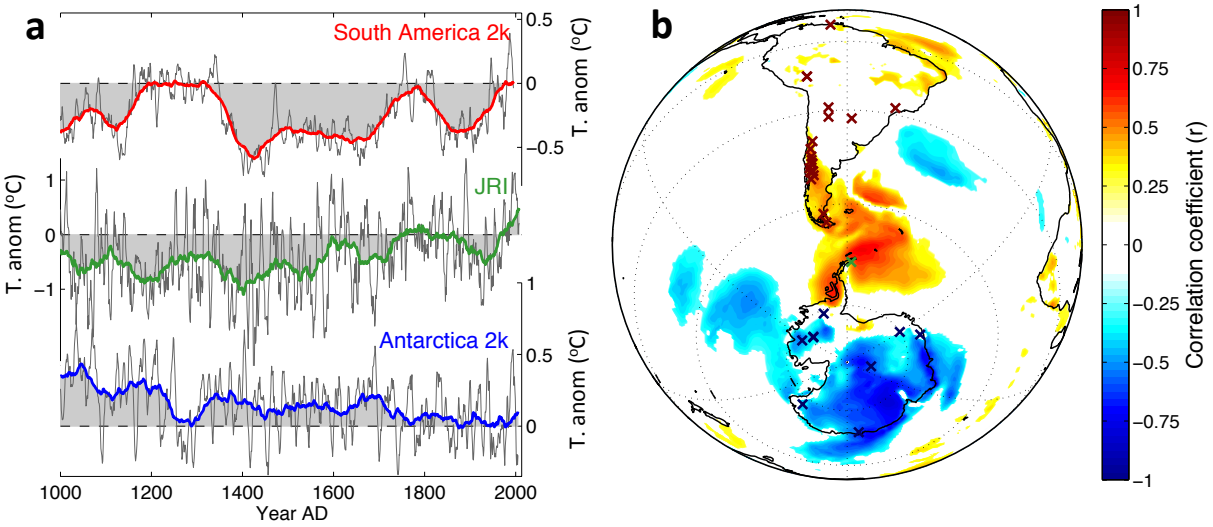
a
South America 2k
JRI
Antarctica 2k
T. anom (°C)
T. anom (°C)
T. anom (°C)
1
0
−1
0.5
0
−0.5
1
0.5
0
1000
1200
1400
1600
1800
2000
Year AD
b
1
0.75
0.5
0.25
0
−0.25
−0.5
−0.75
−1
Correlation coefficient (r)

Figure 1.

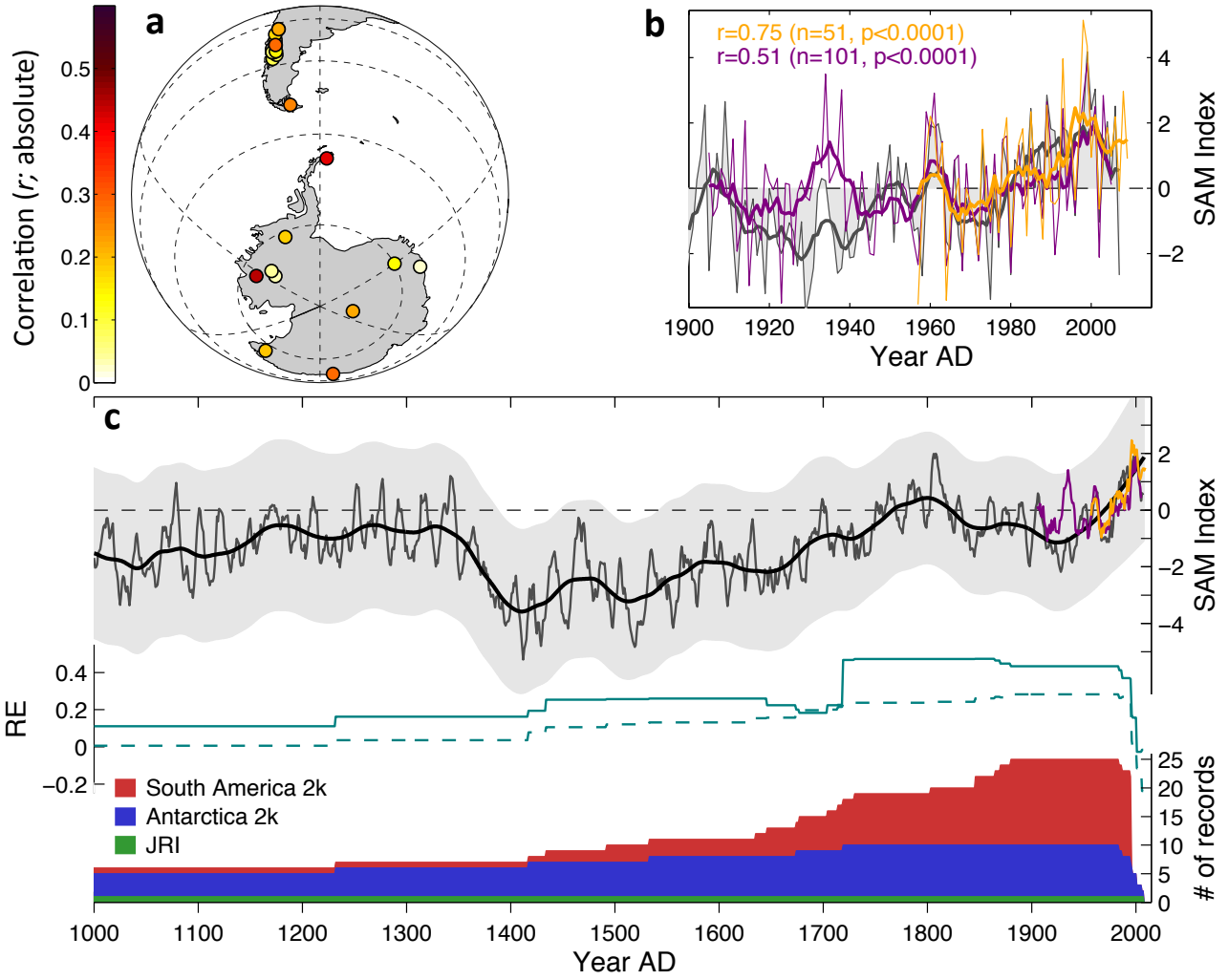
a
Correlation (r; absolute)
0
0.1
0.2
0.3
0.4
0.5
b
r=0.75 (n=51, p<0.0001)
r=0.51 (n=101, p<0.0001)
SAM Index
4
2
0
−2
1900
1920
1940
1960
1980
2000
Year AD
c
SAM Index
2
0
−2
−4
RE
0.4
0.2
0
−0.2
South America 2k
Antarctica 2k
JRI
# of records
25
20
15
10
5
0
1000
1100
1200
1300
1400
1500
1600
1700
1800
1900
2000
Year AD

Figure 2.

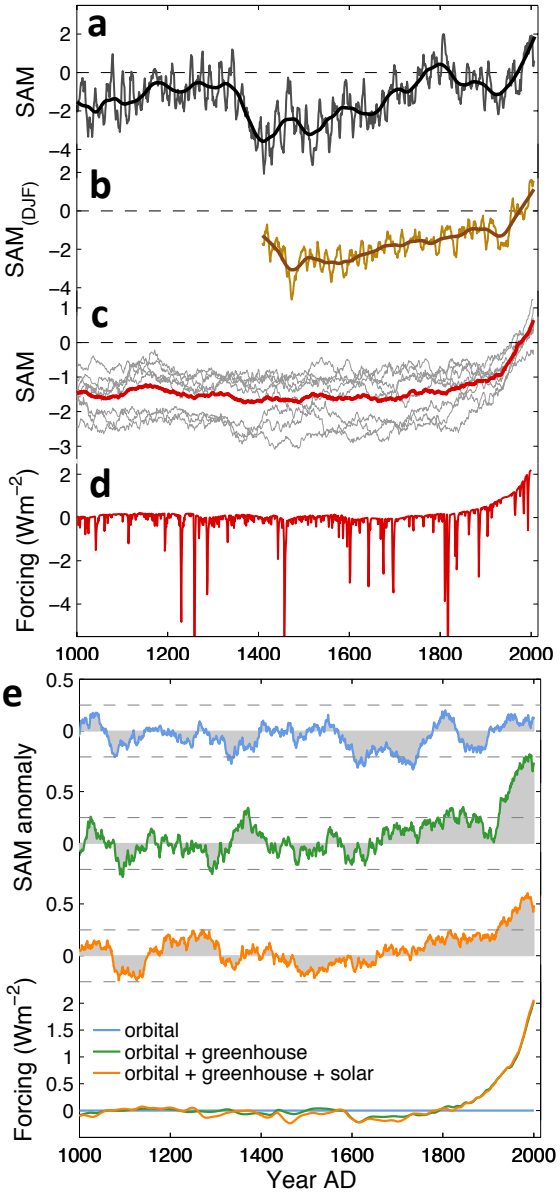
a
SAM
b
SAM(DJF)
c
SAM
d
Forcing (Wm−2)
1000
1200
1400
1600
1800
2000
e
SAM anomaly
Forcing (Wm−2)
orbital
orbital + greenhouse
orbital + greenhouse + solar
Year AD

Figure 3.

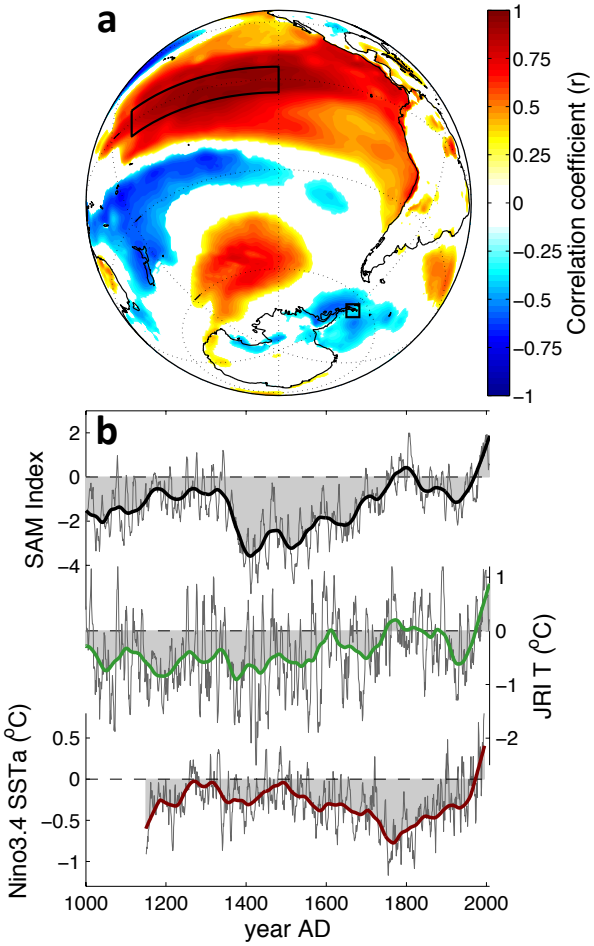
a
1
0.75
0.5
0.25
0
−0.25
−0.5
−0.75
−1
Correlation coefficient (r)
b
SAM Index
2
0
−2
−4
JRI T (°C)
1
0
−1
−2
Nino3.4 SSTa (°C)
0.5
0
−0.5
−1
1000
1200
1400
1600
1800
2000
year AD

Figure 4.